Carcinogenesis vol.35 no.4 pp.867–876, 2014
doi:10.1093/carcin/bgt398
Advance Access publication November 30, 2013

Reduced expression of the chromatin remodeling gene *ARID1A* enhances gastric cancer cell migration and invasion via downregulation of E-cadherin transcription

Hai-Bo Yan[1,2,†], Xue-Fei Wang[3,†], Qian Zhang[1,2,†], Zhao-Qing Tang[3], Ying-Hua Jiang[2], Hui-Zhi Fan[4], Yi-hong Sun[3], Peng-Yuan Yang[2,4] and Feng Liu[1,2,*]

[1]School of Life Sciences and School of Basic Medical Sciences, Fudan University, 131 Dongan Road, Shanghai 200032, China, [2]Institutes of Biomedical Sciences, Fudan University, 130 Dongan Road, Shanghai 200032, China, [3]Department of General Surgery, Zhongshan Hospital, Fudan University, Shanghai 200032, China and [4]Department of Chemistry, Fudan University, 220 Handan Road, Shanghai 200433, China

*To whom correspondence should be addressed. Tel: +86 21 54237451; Fax: +86 21 54237451;
Email: liuf@fudan.edu.cn
Correspondence may also be addressed to Yi-hong Sun.
Email: yihongsun@medmail.com.cn

The chromatin remodeling gene AT-rich interactive domain-containing protein 1A (*ARID1A*) encodes the protein BAF250a, a subunit of human SWI/SNF-related complexes. Recent studies have identified *ARID1A* as a tumor suppressor. Here, we show that *ARID1A* expression is reduced in gastric cancer (GC) tissues, which are significantly associated with local lymph node metastasis, tumor infiltration and poor patient prognosis. *ARID1A* silencing enforces the migration and invasion of GC cells, whereas ectopic expression of *ARID1A* inhibits migration. The adhesive protein E-cadherin is remarkably downregulated in response to *ARID1A* silencing, but it is upregulated by *ARID1A* overexpression. E-cadherin overexpression significantly inhibits GC cell migration and invasion, whereas *CDH1* (coded E-cadherin) silencing promotes migration. Restored expression of *CDH1* in *ARID1A*-silenced cell lines restores the inhibition of cell migration. Luciferase reporter assays and chromatin immunoprecipitation indicate that the ARID1A-associated SWI/SNF complex binds to the *CDH1* promoter and modulates *CDH1* transcription. *ARID1A* knockdown induces evident morphological changes of GC cells with increased expression of mesenchymal markers, indicating an epithelial–mesenchymal transition. *ARID1A* silencing does not alter the level of β-catenin but induces a subcellular redistribution of β-catenin from the plasma membrane to the cytoplasm and nucleus. Immunohistochemical studies demonstrate that reduced expression of E-cadherin is associated with local lymph node metastasis, tumor infiltration and poor clinical prognosis. ARID1A and E-cadherin expression show a strong correlation in 75.4% of the analyzed GC tissues. They are synergistically downregulated in 23.5% of analyzed GC tissues. In conclusion, *ARID1A* targets E-cadherin during the modulation of GC cell migration and invasion.

Introduction

The AT-rich interactive domain-containing protein 1A (*ARID1A*) gene encodes BRG1-associated factor 250a (BAF250a), a non-catalytic subunit of the SWItch/Sucrose Non-Fermentable (SWI/SNF) chromatin remodeling complex (1). This complex plays several important roles in a variety of biological processes including tumor progression. The mammalian SWI/SNF complex contains several subunits, including a core catalytic subunit encoded by Brahma-related gene-1 or the mammalian homolog of *Drosophila brahma* (BRM), as well as 8–10 other Brahma-related gene-1- or BRM-associated factors (BAFs) (1,2). *ARID1A* is frequently mutated in a wide variety of human cancers, as revealed by several genome-wide sequencing studies (3,4). High rates of *ARID1A* mutation were observed in 46–57% of ovarian clear-cell carcinomas, 30% of endometrioid carcinomas (5,6) and 17% of Burkitt lymphomas (7). In liver cancer, *ARID1A* mutations were observed in 10–16.8% of the studied tumors (8,9) and in 13% of hepatitis B virus-associated hepatocellular carcinomas (10). Chromosomal deletions and sequence alterations of *ARID1A* and *ARID1B* were identified in 11% of childhood cancer neuroblastomas (11). *ARID1A* was mutated in 8% of lung cancers and showed a significant accumulation of nonsense substitutions and frameshift insertions and deletions (12). Mutations of *ARID1A* were also found in endometrial tumors (13), renal carcinoma (14), bladder cancer (15), large B-cell lymphoma (16), Barrett's esophagus (17), colon and rectal cancer (18) and pancreatic cancer (19). In gastric cancers (GCs), frequent inactivating mutations or protein deficiencies of *ARID1A* were found to be significantly associated with microsatellite instability and Epstein-Barr virus infection (20,21).

ARID1A frameshift and nonsense mutations are considered to be the primary causes of reduced ARID1A expression. These types of mutations will inevitably lead to mRNA decay, incorrect protein folding or functional defects via deficient domains. Consequently, losses of ARID1A expression are frequently observed in various cancer types, with most known cases reported in gynecologic cancers (4,22). These findings suggest that *ARID1A* is a candidate tumor suppressor.

Functional studies have revealed that decreased expression of ARID1A is associated with poor prognosis in primary GCs (21,23). Silencing of *ARID1A* in cultured GC cell lines enhances proliferation and colony formation, whereas restoring *ARID1A* expression exerts the reverse effect. Furthermore, *ARID1A* silencing facilitates the migration and invasion of liver cancer cell lines (10). Restoration of *ARID1A* expression in the breast cancer cell line T47D significantly inhibits colony formation in soft agar (24). Further analyses indicate that BAF250a collaborates with p53 to regulate *cyclin-dependent kinase inhibitor 1A* (*CDKN1A*) (p21) and *SMAD family member 3* (*SMAD3*) transcription and tumor growth in gynecologic cancers (22). *ARID1A* directly represses *E2F transcription factor 1* (*E2F1*), a cell-cycle regulator (25). *ARID1A* silencing increases mRNA levels of *E2F1* and *cyclin E1* (*CCNE1*) (21). The *c-MYC* gene is also a downstream target of ARID1A (26,27). These results suggest that ARID1A at least partially suppresses cell proliferation by modulating the expression of genes associated with the cell cycle. In several cases, *ARID1A* mutation or expression occurs in a synergistic or exclusive fashion with other genes, such as *phosphatidylinositol-4,5-bisphosphate 3-kinase, catalytic subunit alpha* (*PIK3CA*), *TP53* and *SWI/SNF related, matrix associated, actin-dependent regulator of chromatin, subfamily a, member 4* (*SMARCA4*) (20,21,28). Several lines of evidence suggest that the elevated proliferation of cancer cells induced by low expression of ARID1A is associated with the activation of the phosphatidylinositol 3-kinase (PI3K) pathway (29,30). Collectively, these findings suggest a tumor suppression model of ARID1A through modulation of cell-cycle genes and the PI3K pathway.

However, the underlying molecular mechanisms that link reduced expression of *ARID1A* to enhanced cancer cell migration and invasion remain unknown. In this study, we demonstrate that *ARID1A* knockdown enhances GC cell migration and invasion and reduces the expression of E-cadherin. Restoring wild-type expression levels of *ARID1A* upregulates E-cadherin expression through the regulation

Abbreviations: ARID1A, AT-rich interactive domain-containing protein 1A; BAF250a, BRG1-associated factor 250a; CDH1, *cadherin 1*; ChIP, chromatin immunoprecipitation; GC, gastric cancer; HR, hazard ratio; IHC, immunohistochemistry; PI3K, phosphatidylinositol 3-kinase; qPCR, quantitative reverse transcription PCR; shRNA, short hairpin RNA; SWI/SNF, SWItch/Sucrose Non-Fermentable; TMAs, tissue microarrays.

[†]These authors contributed equally to this work.

of the *cadherin 1* (*CDH1*) promoter, which significantly suppresses GC cell migration and invasion. Consequently, silencing of E-cadherin enhances GC cell migration. *ARID1A* knockdown induces changes in GC cell morphology and the relocation of β-catenin from the plasma membrane to the cytoplasm and nucleus. BAF250a and E-cadherin expression are found to be regulated in a coordinated fashion, and their reduced expression is associated with poor prognosis of GC patients.

Materials and methods

Cell culture

The GC cell lines HGC-27, BGC-823 and MGC-803 were purchased from Cell Bank of Shanghai, Institutes for Biological Sciences, China. The cell line SGC-7901 was a gift from Dr Jian-Jun Du. GES-1 and AGS were generously provided by Dr Qing-Hua Zhang. GC cells were cultured in RPM 1640 media supplemented with 10% fetal bovine serum in a humidified incubator at 37°C and 5% CO_2. HEK293FT was cultured in Dulbecco's Modified Eagle's Medium supplemented with 10% fetal bovine serum.

Antibodies

BAF250a antibody (HPA005456) was purchased from Sigma-Aldrich. E-cadherin antibody (no. ab15148, Abcam) was used for immunohistochemistry (IHC) analysis. Antibodies for human E-cadherin (no. 3195S) and β-catenin were purchased from Cell Signaling Technology. GAPDH antibody was purchased from Kangwei Century Co. LTD, Beijing, China.

Gene cloning and lentivirus production

A synthesized fragment of the 5′ coding sequence of *ARID1A* (2358 bp) was inserted into the Xba I (vector)-Kpn2 I (gene) site of plasmid CMV-T7-hOsa1 (Addgene plasmid 17986), which harbors a partial *ARID1A* coding sequence (6400 bp). The full coding sequence of *ARID1A* was amplified from this vector and subcloned into pcDNA 3.1 (−) for the overexpression assay.

The full-length *CDH1* (E-cadherin) gene was amplified by reverse transcription PCR using total RNA extracted from the gastric cell line GES-1 and inserted into pcDNA 3.1 for the overexpression assay.

The short hairpin RNA (shRNA) lentiviral plasmid (pLKO.1) was obtained from The RNA Interference (RNAi) Consortium. The shRNA sequences for *ARID1A* are listed in Supplementary Table 1, available at *Carcinogenesis* Online. Lentivirus was produced using HEK293FT cells with the second-generation packaging system psPAX2 (Addgene plasmid 12260) and pMD2.G (Addgene plasmid 12259). Lentiviral titer was determined by a real-time quantitative method by measuring viral RNA content in viral supernatant as described (31).

Cell transfection

All transfections were performed using Lipofectamine 2000 (Life Technologies—Invitrogen) following the manufacturer's instructions with minor modifications. Briefly, 2 μg plasmid DNA or 6 μl siRNA was added to OPTI-MEM reduced serum media (Life Technologies—Invitrogen) for a final volume of 200 μl. The mixture was incubated for 5 min at room temperature. Next, 2 μl lipofectamine was combined with 200 μl OPTI-MEM and incubated for 5 min at room temperature. These stocks were combined and kept at room temperature for 20 min before transfection of target cells. Target cell culture medium was changed 6 h after transfection. The sequences of *ARID1A* siRNAs were synthesized according to Wang *et al.* (23) and listed in Supplementary Table 1, available at *Carcinogenesis* Online.

RNA extraction and quantitative reverse transcription PCR

Total RNA was isolated using TRIzol reagent (Life Technologies—Invitrogen). First strand cDNA was generated using the PrimeScript 1st Strand cDNA Synthesis Kit (Takara Bio Inc.), and quantitative reverse transcription PCR (qPCR) was performed using the IQ5 Real-Time PCR detection system (Bio-Rad) with SYBR green (Takara Bio Inc.). Primers are listed in Supplementary Table 1, available at *Carcinogenesis* Online.

Western blot analysis

Cultured cells and tissue samples were lysed using radioimmunoprecipitation buffer and T-PER tissue protein extraction reagent (Thermo Scientific Pierce) in the presence of a protease inhibitor cocktail (Roche Applied Science). Protein concentration was quantified using a BCA protein assay kit (Thermo Scientific Pierce). Proteins were separated by 12.5% sodium dodecyl sulfate–polyacrylamide gel electrophoresis and transferred onto an Immobilon-P Transfer membrane (Merck Millipore). Immunoblots were performed by standard protocol. Chemiluminescence was developed using SuperSignal West Femto Maximum Sensitivity Substrate (Thermo Scientific Pierce). Signals were detected with a LAS-3000 imager (Fujifilm). GAPDH was detected using mouse anti-human GAPDH monoclonal antibody (1:3000 dilution) as a loading control.

Cell migration and invasion assay

Migration of GC cells was assessed using the QCM™ 24-well colorimetric cell migration assay kit (BD Biosciences) according to the manufacturer's instructions. Briefly, GC cell lines were transfected with siRNA and were incubated in serum-free medium for 24 h. The cells were then transferred to the upper chamber of a Transwell plate by seeding 1×10^5 cells per well in 200 μl serum-free medium. Next, 0.5 ml 10% fetal bovine serum-containing medium was added to the lower chamber as a chemoattractant. Cells were incubated for 16–24 h (depending upon the migration ability of cells) at 37°C. Non-migrating cells on the upper membrane surface were scraped off with cotton swabs. Cells that migrated to the bottom of the membrane were stained with 0.1% crystal violet for 10 min, followed by washing with water for 30 s to remove residual dye. The dye was dissolved with 33% acetic acid, and absorbance was measured at 570 nm using a BioTek Epoch Microplate Spectrophotometer. Each experiment was performed in triplicate. The invasion assay was performed in a similar fashion using a cell invasion assay kit (BD Biosciences), except that the upper chambers were precoated with ECMatrix™ gel. Statistical significance was calculated by the Student's *t*-test, and P value < 0.05 was considered significant.

Luciferase activity assay

The promoter region (−289 to +105) of *CDH1* was amplified using normal human genomic DNA and inserted into the pGL3 luciferase reporter vector (Promega). GC cells were seeded in 24-well plates and cultured for 16 h before *ARID1A* siRNA transfection. Six hours later, culture medium was changed, and cells were further cultured for 32 h. At this point, cells were transfected by wild-type or E-box mutant *CDH1* luciferase constructs in addition to a Renilla vector used as an internal control for luciferase activity. After 2 days of incubation, luciferase assays were conducted using the dual luciferase assay system (Promega). Each experiment was performed in triplicate.

5-Azacytidine treatment

GC cells (AGS, BGC-823 and HGC-27) were cultured on 6-well plates (Corning). After 24 hours, the demethylation agent 5-azacytidine was added to the culture medium at a concentration of 10 μM. After 5-azacytidine treatment for 30 h, cells were harvested, and RNA was extracted and analyzed by qPCR.

Chromatin immunoprecipitation

The chromatin immunoprecipitation (ChIP) assay was performed using an EZ-ChIP kit (17–371, Upstate Biotechnology) according to manufacturer's instructions and a previous publication (32). Briefly, cells were cross-linked with 1% formaldehyde (Sigma-Aldrich), and cell lysate was sonicated to shear DNA. For each experiment, chromatin was precipitated using 5 μg antibody (anti-ARID1A or normal mouse IgG) preabsorbed onto 60 μl protein G agarose. Reaction was performed overnight at 4°C with agitation. After reverse cross-linking, the DNA was purified according to the manufacturer's instructions. The E-cadherin promoter region located −245 to −91 bp upstream of the transcription start site was amplified, and products were quantified by qPCR using both the ChIP-enriched DNA and input DNA as template. Enrichment by ChIP was assessed relative to the input DNA and normalized to the level of GAPDH. The PCR primers are listed in Supplementary Table 1, available at *Carcinogenesis* Online.

Subcellular fractionation

To analyze the subcellular redistribution of β-catenin after *ARID1A* silencing, GC cells were fractionated into plasma membrane and cytosol/nuclear portions using a Membrane and Cytosol Protein Extraction Kit (P0033, Beyotime Inc., Haimen, China) according to the manufacturer's instructions. Subcellular proteins were extracted, and western blots were carried out with E-cadherin and β-catenin antibodies.

Human tissue samples and tissue microarray

We used 60 paired cancerous and gastric mucosa tissues for qPCR analyses of *ARID1A* and *CDH1* genes. The samples were collected at Zhongshan Hospital of Fudan University, and signed informed consent was obtained from all patients. The study was approved by the Clinical Research Ethics Committee of Zhongshan Hospital of Fudan University.

The expression of ARID1A and E-cadherin was analyzed using two tissue microarrays (TMAs). One of the TMAs was prepared by Zhongshan Hospital of Fudan University as described previously (33,34), containing 108 pairs of tumor and adjacent normal samples. The samples include 79 adenocarcinomas, 21 tubular adenocarcinomas, 5 mucinous adenocarcinomas, and 3 signet ring cell carcinomas. Follow-up information was unavailable for 7 of the 108 cases. The IHC experiments and interpretations were independently performed twice by histopathology experts.

Commercial TMA was also used (catalog no.HStm-Ade167Sur-01, Shanghai Outdo Biotech, China), consisting of 75 paired GC and paraneoplastic tissues, 8 GCs and 9 normal paraneoplastic mucosa tissues. The paired 75 GC samples include 53 adenocarcinomas, 16 tubular adenocarcinomas, 4 mucinous

adenocarcinomas and 2 signet ring cell carcinomas. Patient follow-up information was available from 2006 to 2011. Each section was stained according to a commercial protocol (Outdo Biotech), followed by scanning with Scanscope XT (Aperio).

IHC and statistics

Tissue sections (4 μm) were incubated overnight in a 56°C oven. After deparaffinization and rehydration, antigen retrieval was performed by boiling sections in 10 mM citrate buffer (pH 6.0) for 25 min. Endogenous peroxidase activity was inactivated using 0.3% H_2O_2 for 15 min at room temperature. The sections were blocked with 3% BSA in PBS for 30 min and subsequently incubated with primary antibodies. The immune complex was visualized using a Dako REAL™ Envision™ Detection system. Nuclei were counterstained with hematoxylin. The correlation of BAF250a or E-cadherin expression and clinicopathological characteristics were evaluated by χ^2 test using R language. Kaplan–Meier survival curves were calculated using the log-rank test with GraphPad Prism 5. P value < 0.05 is considered statistically significant.

Results

Reduced expression of ARID1A in GC patients associated with poor prognosis and metastasis

As revealed by qPCR, *ARID1A* mRNA levels were significantly downregulated in GCs compared with paraneoplastic normal tissues (n = 60, Student's t-test, P < 0.0001) (Figure 1A). IHC assays using two TMAs revealed that negative expression of BAF250a was evident in 44 out of 183 (24%) GC patients compared with their normal counterparts. Patients with low BAF250a expression showed a significantly worse prognosis than those with high BAF250a expression after gastrectomy (log-rank test, n = 176, P = 0.023) (Figure 1B). Strong BAF250a-positive nuclear staining was found in normal tissues (Figure 1C). Low BAF250a levels were significantly correlated with tumor infiltration (X^2 test, P = 0.012) (Supplementary Table 2, available at *Carcinogenesis* Online). Such results reinforce previous findings in GC (23,35). We also found that the negative staining of BAF250a was significantly associated with local lymph node metastasis (P = 0.004). Univariate analyses of the 176 paired GC cases indicated that higher risk of death is significantly related to larger tumor size (≥ 3 cm) with a hazard ratio (HR) of 1.98 (P = 0.0035) (Supplementary Table 3, available at *Carcinogenesis* Online). Furthermore, risk of death increases significantly along with the progression of local lymph node metastasis (HR ranging from 4.1 to 133.8, $P \leq 0.008$), tumor infiltration (HR ranging from 7.0 to 4.9, $P < 0.0001$) and grade (HR ranging from 4.5 to 5.7, $P \leq 0.0005$) (Supplementary Table 3, available at *Carcinogenesis* Online). Higher risk of death is also significantly associated with the loss of ARID1A (HR = 1.98, P = 0.0255). These findings suggest that loss of ARID1A is associated with poor prognosis and metastasis. ARID1A may play an essential role in the suppression of GC tumorigenesis and metastasis.

ARID1A knockdown promotes GC cell migration and invasion, whereas ectopic expression of ARID1A inhibits GC cell migration

ARID1A has been shown to suppress hepatocellular carcinoma cell migration and invasion (10), whereas its role in GCs remains unknown. To analyze the function of *ARID1A* in GC cells, we silenced *ARID1A* in GC cell lines MGC-803, HGC-27 and SGC-7901 by transient transfection with *ARID1A* siRNA or control siRNA. We also stably silenced *ARID1A* in HGC-27 cells. As shown in Figure 2A, *ARID1A* was downregulated using both siRNA or shRNA. Migrations of all three GC cell lines were significantly enhanced after *ARID1A* knockdown (P = 0.0006 for MGC-803, P

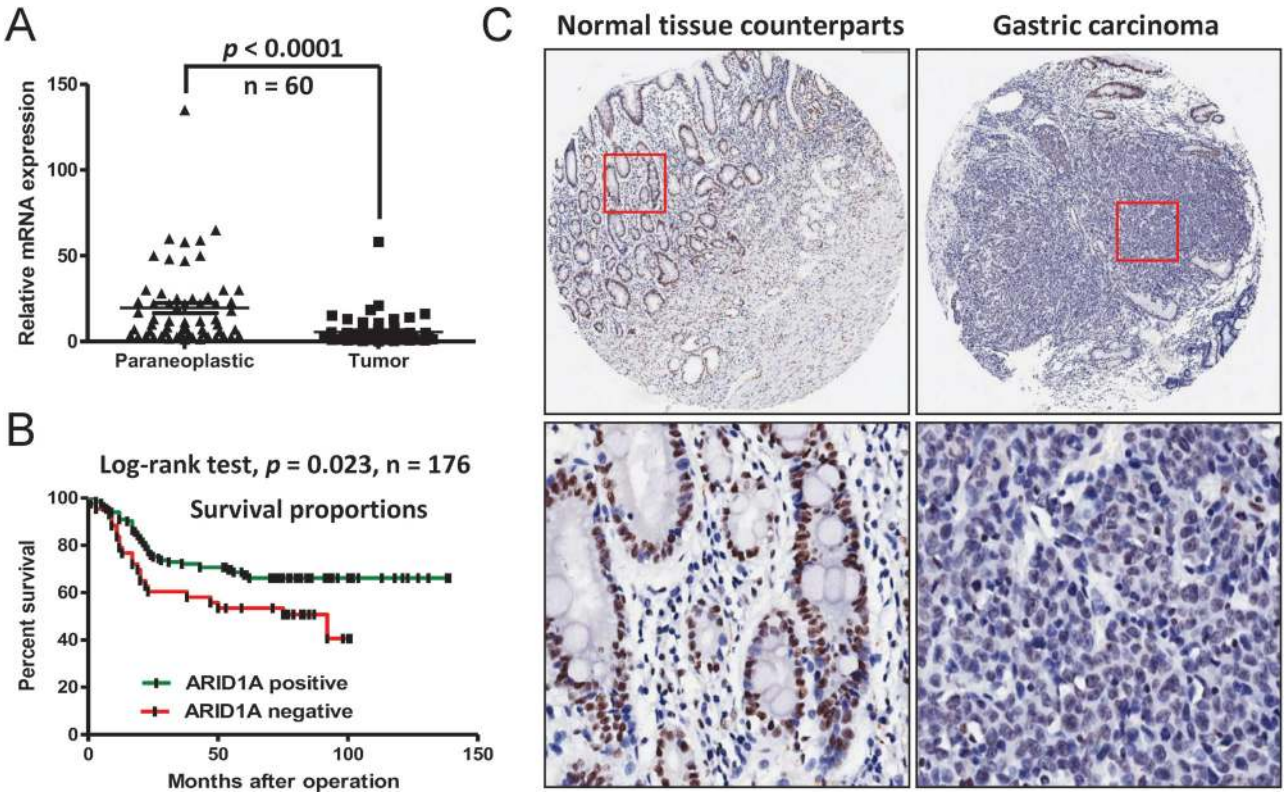

Fig. 1. Recurrent reduction of ARID1A expression in gastric carcinoma was associated with poor prognosis. (**A**) mRNA level of *ARID1A* was quantified with qPCR in 60 paired GC and paraneoplastic normal tissues. Horizontal lines indicate the median of biological replicates (n = 60). Significant differences between normal and cancer tissue were calculated by Student's t-test (P < 0.0001). (**B**) Kaplan–Meier survival curves of GC patients (n = 176, 75 from Outdo Biotech and 101 from Zhongshan) after gastrectomy. Patients with low BAF250a expression had a significantly worse prognosis than those with high BAF250a expression (log-rank test, P = 0.023). (**C**) Immunohistochemistry of BAF250a protein expression in GC surgical specimens (from Outdo Biotech). Strong BAF250a-positive staining in normal tissue is shown in the upper-left corner, whereas BAF250a-negative staining in gastric adenocarcinoma is presented in the upper-right corner. Red boxes indicate the area enlarged in the lower panel.

= 0.0008 for HGC-27 and P = 0.005 for SGC-7901) (Figure 2A). In line with the results of transient silencing, stable knockdown of *ARID1A* by shRNAs enhanced GC cell migration significantly (P = 3.6E−5) (Figure 2B). Furthermore, we found that ectopic expression of wild-type full-length *ARID1A* in AGS cells significantly inhibited cell migration in the transwell assay (P < 0.0001) (Figure 2C). Next, we investigated the role of *ARID1A* in an invasion process by ECMatrix assay. We found that siRNA-mediated endogenous *ARID1A* silencing in HGC-27 significantly upregulated cell invasion ability (P = 0.0007) (Figure 2D). Stable silencing of *ARID1A* in AGS cells by shRNAs also enhanced cell invasion (P = 0.02 (sh2), 0.007 (sh3)) (Figure 2E).

ARID1A suppresses GC cell migration by modulation of E-cadherin

ARID1A was shown to suppress cancer cell migration and invasion. However, the underlying molecular mechanism remains unclear.

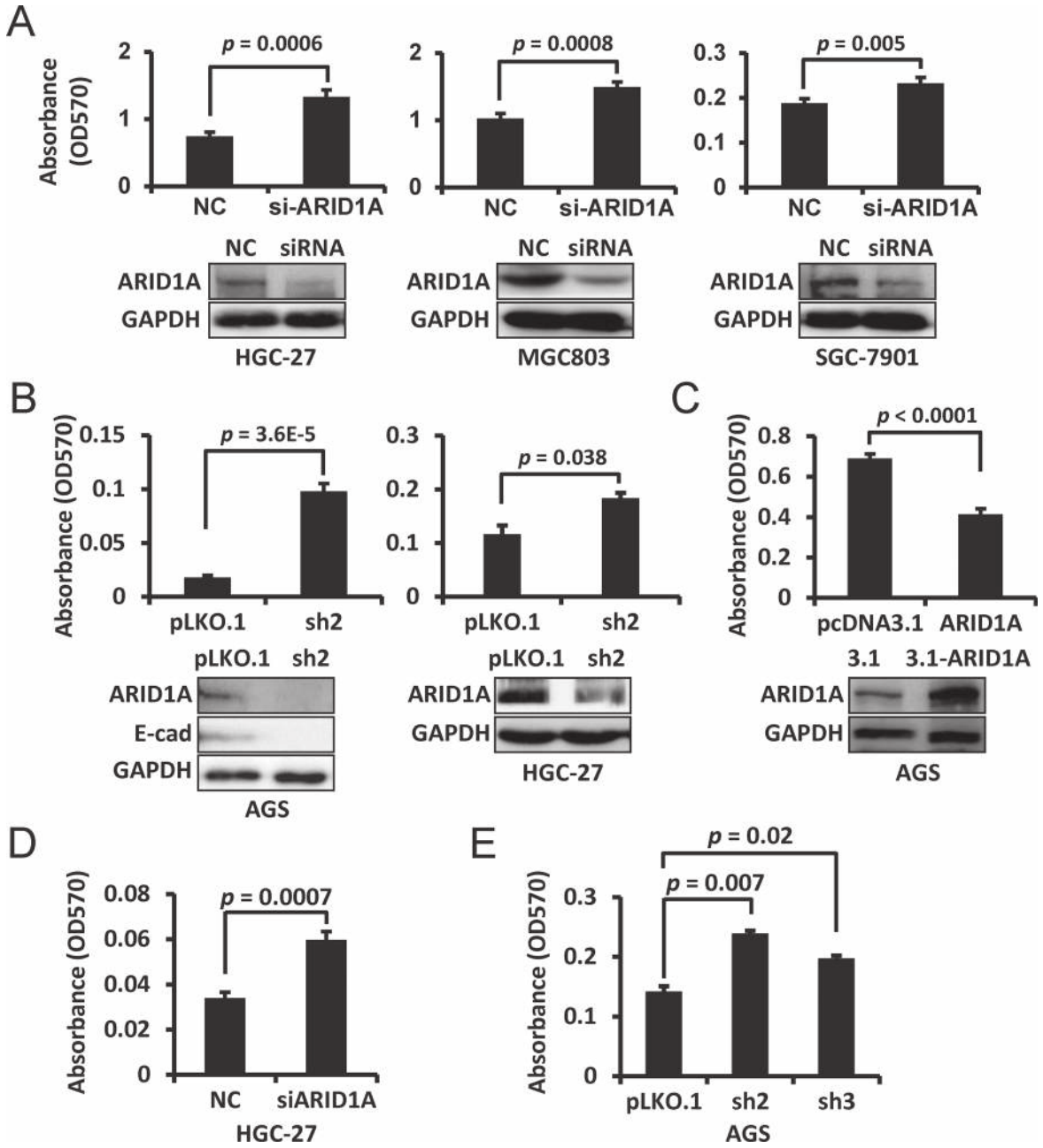

Fig. 2. Silencing of *ARID1A* promotes GC cell migration and invasion, whereas overexpression of *ARID1A* inhibits GC cell migration. (**A**) Cell migration ability changes after *ARID1A* silencing. After transfection of *ARID1A* or negative control siRNA (NC), cells were cultured for 30–48 h before being transferred to the upper chamber of transwell, where the cells were further cultured for 18–24 h. Cells that migrated to the bottom of the membrane were stained by crystal violet and were photographed. Crystal violet was then dissolved with 33% acetic acid, and absorbance was read under OD570. The experiment was performed in triplicate, and P values shown above the bars were calculated by the Student's t-test. P < 0.05 was considered significant. ARID1A expression was analyzed by western blot, as shown under each bar chart. (**B**) Stable shRNA-mediated knockdown of *ARID1A* stimulated GC cell migration. An additional blot shows that the expression of E-cadherin was downregulated by *ARID1A* silencing. (**C**) Cell migration ability changes after *ARID1A* overexpression. The full-length *ARID1A* gene was inserted into pcDNA3.1, which was then used to transfected AGS cells. Migration of AGS cells was significantly reduced by overexpression of *ARID1A* in the transwell assay. (**D**) *ARID1A* was silenced by siRNA in HGC-27 cells, and cell invasion ability was evaluated by ECMatrix invasion assay. The methods for absorbance detection and statistic calculation are the same as the migration assay. (**E**) *ARID1A* was stably silenced in AGS cells by shRNAs, and invasion ability of AGS cells was monitored by ECMatrix invasion assay.

Cell adhesion proteins play an important role in cancer cell migration, invasion and metastasis and are found to be frequently mutated in GC as revealed by exome sequencing (21). Mutations of *CDH1* (E-cadherin), *CTNNB1* (β-catenin) and other genes are known to contribute to gastric carcinogenesis (36). Here we found that E-cadherin expression decreased remarkably in response to stable knockdown of *ARID1A* by shRNAs in the GC cell lines AGS, HGC-27, SGC-7901 and MGC-803 (Figures 2B and 3A). Furthermore, E-cadherin levels were elevated when we overexpressed *ARID1A* in BGC-823 and AGS cells (Figure 3B).

mRNA levels of *CDH1* in HGC-27 cells were analyzed by qPCR after silencing of *ARID1A* with shRNAs. Expression of *CDH1* was significantly downregulated ($P < 0.0001$) compared with control transfections with pLKO.1 (Figure 3C). The above results indicated that *ARID1A* may modulate *CDH1* gene transcription.

The E-cadherin promoter was known to be occasionally methylated in GC or other cancer types (37). However, we found that *CDH1* expression in AGS, HGC-27 and BGC-823 cells was not altered noticeably by treatment of 5-azacytidine, a demethylating agent. This suggests that *CDH1* transcription in these cell models was not manipulated by promoter methylation or demethylation (Supplementary Figure 1, available at *Carcinogenesis* Online). This may exclude the possibility that *ARID1A* regulates *CDH1* transcription through methylation modification. In order to elucidate this mechanism, the *CDH1* promoter was cloned and a luciferase reporter assay was performed to test the binding of BAF250a to the *CDH1* promoter. Interestingly, we found that luciferase activity was significantly reduced by *ARID1A* silencing in SGC-7901 ($P = 0.0032$, *t*-test) and HGC-27 ($P < 0.0001$) (Figure 3D). This result suggests that BAF250a modulated E-cadherin transcription by interaction with the *CDH1* promoter.

ARID1A-DNA interactions are necessary for promoter occupancy by the SWI/SNF complex (38). ARID1A participates in forming SWI/SNF chromatin remodeling complexes and acts to bind to its target genes, such as p21 (22). Therefore, ARID1A may regulate *CDH1* transcription through the binding on its promoter as a subunit of the SWI/SNF complex. To test this hypothesis, we stably silenced endogenous

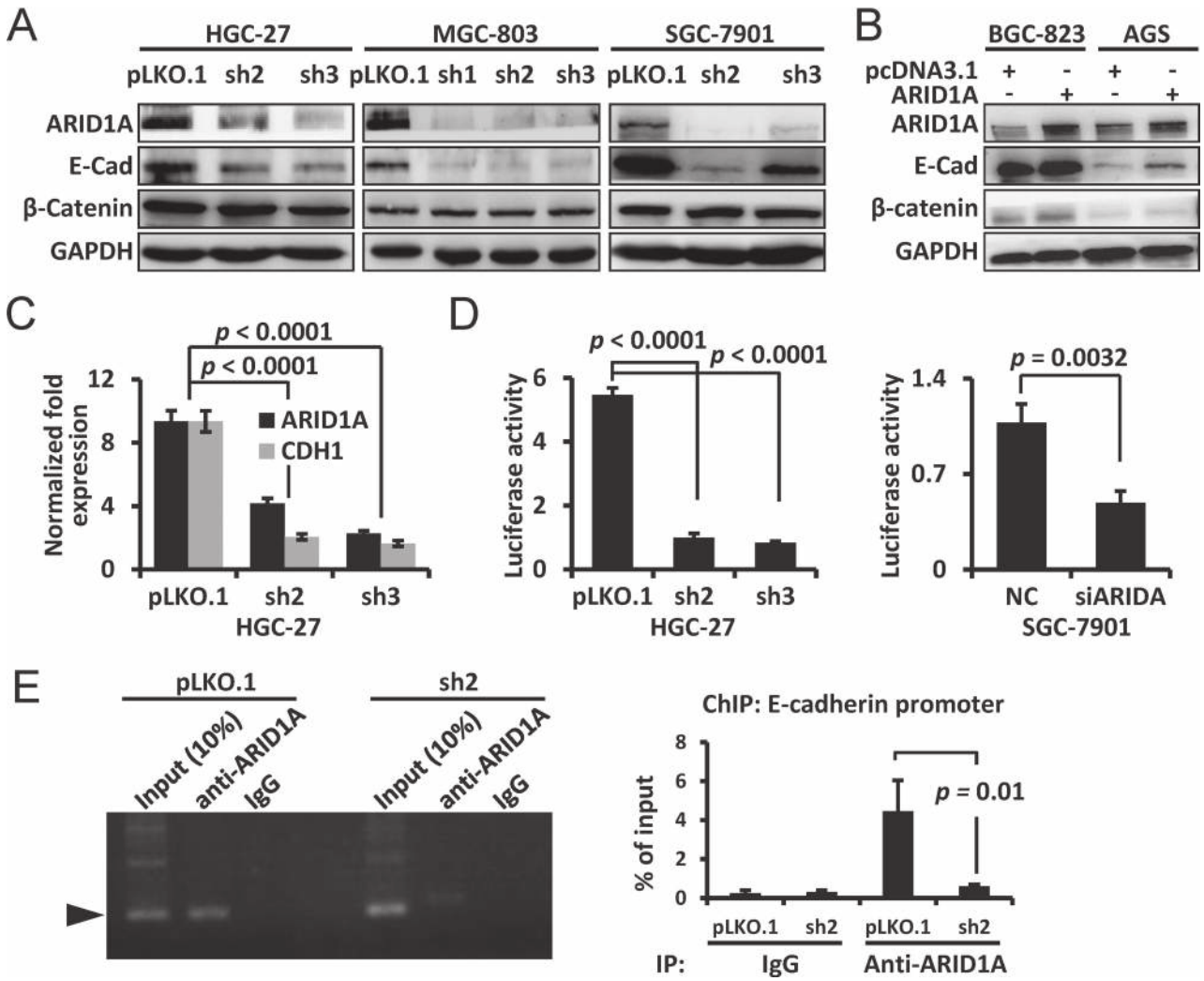

Fig. 3. E-cadherin is a downstream target of ARID1A. (**A**) *ARID1A* was stably downregulated by shRNAs in HGC-27, MGC-803 and SGC-7901 cells. Western blots were performed using indicated antibodies. E-cadherin expression decreased in response to *ARID1A* knockdown, whereas the expression of β-catenin remained unchanged. (**B**) Full-length gene of wild-type *ARID1A* was ectopically expressed in BGC-823 and AGS cells, and western blot was performed using indicated antibodies. (**C**) The mRNA levels of *ARID1A* and *CDH1* (coding E-cadherin) in HGC-27 cells were analyzed by qPCR after silencing of *ARID1A* with shRNAs. (**D**) Luciferase reporter assay of *CDH1* promoter by *ARID1A* silencing. A 394 bp fragment of the 5′ promoter region of *CDH1* was inserted upstream of a luciferase reporter gene in plasmid pGL3. This reporter plasmid was used to transfect HGC-27 cells, where *ARID1A* was stably silenced by shRNA. In addition, the reporter plasmid and siRNA of *ARID1A* were used to transfect SGC-7901 cell lines and reporter expression was quantified. *P* values were calculated by Student's *t*-test. (**E**) ChIP assay was performed in HGC-27 cells where *ARID1A* was stably silenced by shRNA. Chromatin was precipitated using antibodies against ARID1A. Precipitation with IgG served as a negative control. The E-cadherin promoter sequence was amplified and quantified by qPCR. The DNA fragment of E-cadherin promoter is indicated with an arrow head on the gel map (left).

ARID1A by shRNA and performed a ChIP assay to determine changes in SWI/SNF complex binding to the E-cadherin promoter. As shown in Figure 3E, binding of the SWI/SNF complex to the E-cadherin promoter decreased dramatically ($P = 0.01$) when endogenous *ARID1A* was silenced. However, immunoprecipitation using IgG showed quite low signals and no significant changes were detected before and after *ARID1A* silencing. These results suggest that knockdown of *ARID1A* reduces E-cadherin promoter occupancy by the SWI/SNF complex.

GC cell migration was enhanced by silencing of CDH1 gene and inhibited by overexpression of CDH1

We postulate that, as a downstream target of *ARID1A* in gastric cell models, silencing or overexpression of E-cadherin will enhance or suppress cell migration or invasion. We silenced *CDH1* in SGC-7901 and HGC-27 cell lines and revealed that *CDH1* knockdown significantly increased GC cell migration in both cell lines ($P = 0.007$ and $P = 0.005$) (Figure 4A). On the other hand, overexpression of E-cadherin markedly reduced SGC-7901 migration (Figure 4B).

To clarify the relationship between *ARID1A*, E-cadherin and cell migration ability, we performed an E-cadherin rescue assay. In this analysis, we overexpressed E-cadherin in *ARID1A*-silenced GC cell lines. As shown in Figure 4C, *ARID1A* silencing by shRNA reduced E-cadherin expression, whereas additional overexpression of E-cadherin restored partial E-cadherin expression in HGC-27 and SGC-7901 cells. Endogenous *ARID1A* silencing with shRNA significantly enhanced the migration abilities of HGC-27 and SGC-7901 cells. However, when we further overexpressed E-cadherin in the same cell lines, the migration activities of GC cells dropped considerably down to the original levels.

ARID1A silencing induces epithelial–mesenchymal transition of GC cells and the relocation of β-catenin

Interestingly, *ARID1A* knockdown induced evident morphological changes from routine polygonal sharp to spindle sharp morphologies in AGS cells and more protruding filopodia in HGC-27 cells (Figure 5A). Reduction of GC cell surface area decreases cell–cell contact. These morphological changes are accompanied with the downregulation of E-cadherin, an epithelial protein marker. The expression of two typical mesenchymal makers, vimentin and N-cadherin, were elevated after *ARID1A* silencing in HGC-27 and AGS cells (Figure 5B). These observations indicate that *ARID1A* silencing might induce epithelial–mesenchymal transition (EMT) in GC cells.

β-Catenin is known to play dual functions as a member of membrane adhesive molecules in association with E-cadherin and as a member of the Wnt pathway. In the latter case, β-catenin disassociates with E-cadherin and translocates into the nucleus where β-catenin activates LEF-1/TCF transcription, initiating the EMT process (39,40). We found that the expression of β-catenin remained largely stable regardless of *ARID1A* silencing (Figure 3A) but was upregulated slightly along with the increase of E-cadherin, as revealed by western blot analyses (Figure 3B). We extracted plasma membrane and cytosol/nuclear protein fractions and analyzed the distribution of β-catenin. Consistent with above findings, the expression of β-catenin was reduced in the plasma membrane but increased in cytoplasm and nucleus when *ARID1A* was silenced in HGC-27 cells (Figure 5C). Immunofluorescence analyses demonstrated that endogenous E-cadherin and β-catenin are localized on the plasma membrane of HGC-27 cells (Figure 5D). When *ARID1A* was stably silenced in HGC-27 cells, membranous E-cadherin was almost completely diminished, whereas β-catenin was redistributed to the cytoplasm and nucleus. These results indicate that *ARID1A* silencing disrupts the membrane-bound E-cadherin/β-catenin complex and induces a relocation of β-catenin into the nucleus (Figure 5E).

Low expression of E-cadherin in GC tissues is associated with poor clinical prognosis

Next, we analyzed the expression of E-cadherin and its correlation with ARID1A expression in GC tissues. As determined by IHC analyses of the same set of GC TMAs, low expression of E-cadherin was evident in these patients and significantly associated with worse clinical prognosis (log-rank test, $n = 100$, $P = 0.041$) (Figure 6A). Furthermore, reduced expression of E-cadherin was found to be significantly associated with local lymph node metastasis ($P = 0.001$) and tumor infiltration ($P = 0.006$) (Supplementary Table 4, available at *Carcinogenesis* Online). These results are similar to ARID1A (Supplementary Table 2, available at *Carcinogenesis* Online).

We evaluated the transcription levels of both *ARID1A* and *CDH1* by qPCR in 20 pairs of gastric carcinoma and adjacent normal gastric mucosa specimens. Interestingly, *CDH1* transcription levels were found to correlate with *ARID1A* ($R^2 = 0.5138$), calculated as $\log_2$-transformed expression between normal and cancer tissues (Figure 6B). Furthermore, we analyzed the correlation between BAF250a and E-cadherin expression in the same sets of TMAs. By the IHC statistics of 183 paired GC tissues, BAF250a and E-cadherin were expressed in a synergetic fashion in 75.4% (138) GC tissues (X^2 test, $P < 0.0001$) (Supplementary Table 5, available at *Carcinogenesis* Online), including some synergetic downregulations in 43 (23.5%) cases and some synergetic upregulations in 14 (7.7%) GC tissue samples. In normal gastric tissues, BAF250a was expressed predominantly in the nucleus, whereas E-cadherin was expressed in the membranous components of cell–cell junctions (Figure 6C).

Discussion

The *ARID1A* gene has been classified as a novel tumor suppressor, as evidenced by links between ARID1A/BAF250a expression and several gynecologic cancers, including ovarian clear-cell cancers and endometrial carcinomas, stomach cancers as well as breast cancers (41). Loss of *ARID1A* expression is mostly induced by nonsense mutations and insertions and deletions in the gene-coding region, which lead to mRNA decay or sequence truncation (4). A recent study suggests that promoter hypermethylation is also responsible for the reduced expression of *ARID1A* (42). In this study, we also demonstrated that negative expression of ARID1A was common in 30.3% of studied GC patients and was associated with poor clinical prognosis.

ARID1A was reported to suppress tumor cell proliferation by modulation of cell-cycle-related genes, such as *CDKN1A* (p21), *SMAD3*, *C-MYC* and *E2F1*, in a p53-independent fashion (21,22,25). In endometrial cancer, mutations in *ARID1A* are frequently associated with PI3K pathway activation (30,43). Consequently, *ARID1A* overexpression was found to downregulate the phosphorylation of AKT in glioma cells (29). These findings suggest that the PI3K-AKT pathway is activated when *ARID1A* is silenced, and the activation of this pathway might involve in the accelerated proliferation of cancer cells.

ARID1A deficiency has also been associated with enhanced migration and invasion of cancer cells (10). However, the underlying molecular mechanism is still unknown. Here, we revealed by immunohistochemical analyses that reduced expression of ARID1A in GC tissues is significantly associated with tumor infiltration and local lymph node metastasis, reinforcing previous findings (23,35). We found that silencing endogenous *ARID1A* increases GC cell migration and invasion *in vitro*, whereas ectopic expression of wild-type *ARID1A* suppresses GC cell migration.

One of our novel findings is that E-cadherin, an important adhesive molecule involved in the inhibition of cancer migration and invasion (44), is a downstream target of ARID1A. We show evidence that ARID1A interacts with the *CDH1* promoter to modulate its transcription, as revealed by the Luciferase reporter assay. ARID1A cannot regulate the transcription of *CDH1* gene if its promoter is replaced by another promoter (Figure 5C). In addition, chromatin immunoprecipitation indicates that ARID1A might bind directly to the promoter of E-cadherin as a component of the SWI/SNF chromatin remodeling complex. Therefore, the *CDH1* promoter is expected to contain a binding motif for the ARID1A-involved SWI/SNF complex.

To confirm the association of ARID1A and E-cadherin in cancer metastasis, we further analyzed the function of E-cadherin in GC cells and tissues. Ectopic expression of E-cadherin alone significantly

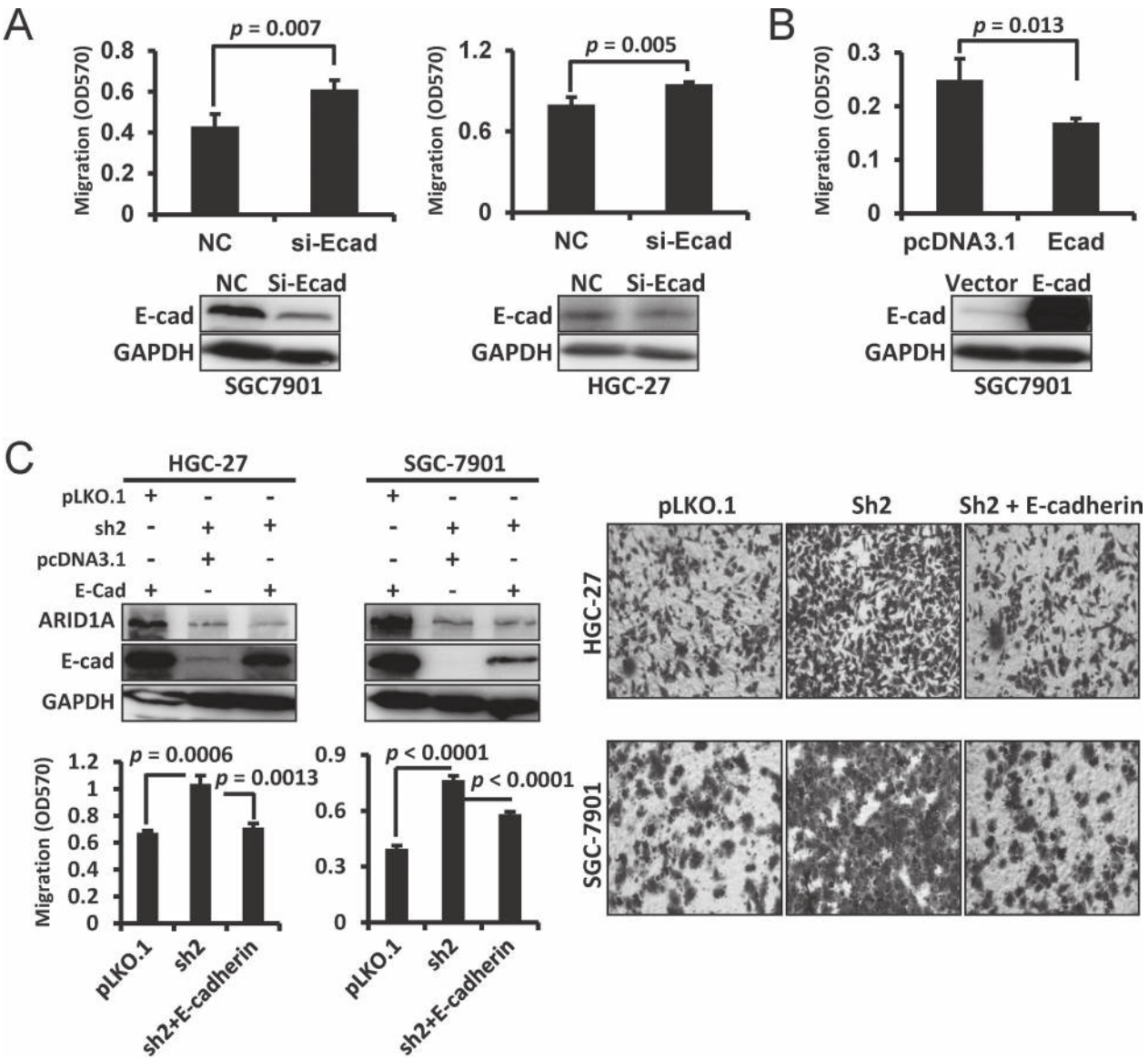

Fig. 4. GC cell migration was enhanced by silencing of *CDH1* but was inhibited by overexpression of *CDH1*. (**A**) SGC-7901 and HGC-27 cell lines were transduced by siRNA for *CDH1* and cultured for 30–48 h. Cells were then transferred to the upper chamber of transwell plates and cultured for an additional 24 h. After this incubation, cells that migrated to the bottom of the membrane were stained by crystal violet and photographed. Crystal violet was then dissolved with 33% acetic acid, and absorbance was read under OD570. Prior to the migration assay, the downregulation of E-cadherin protein was analyzed by western blot as shown in the middle panel. Statistical analysis was conducted between *CDH1* knockdown and control cells by the Student's *t*-test, and *P* values are shown above the bars. (**B**) Migration of SGC-7901 cells was significantly reduced by overexpression of E-cadherin in transwell assay. (**C**) GC cell migration enhanced by *ARID1A* silencing was inhibited by E-cadherin overexpression. *ARID1A* silencing by sh2 and E-cadherin overexpression (E-cad) was verified by western blot shown to the upper left. The effects of *ARID1A* silencing and E-cadherin overexpression on the migratory ability of HGC-27 and SGC-7901 were tested in the transwell assay. Crystal violet was then dissolved with 33% acetic acid, and absorbance was read under OD570. Statistical analysis was performed by Student's *t*-test. Sh2 + E-cadherin, E-cadherin was overexpressed in GC cell lines stably transfected with sh2 of *ARID1A*.

inhibited GC cell migration and invasion *in vitro*, whereas *CDH1* knockdown exerted the reverse effect. Furthermore, restoration of *CDH1* expression in *ARID1A*-silenced cell lines inhibited cell migration. We found that E-cadherin was downregulated in GC tissues, and its downregulation correlates with poor prognosis of GC patients. In a similar fashion to ARID1A, reduced expression of E-cadherin was significantly associated with local lymph node metastasis and tumor infiltration, as is consistent with previous findings (45). The expression of BAF250a and E-cadherin showed strong correlation in GC tissue samples (Figure 6B and C). Interestingly, synergistically reduced expression of ARID1A and E-cadherin was evident in 23.5% of patients. This raises a hypothesis that reduced expression of E-cadherin might be induced by loss of ARID1A expression. In such cases, restoring the expression of *ARID1A* and/or E-cadherin would be an attractive therapeutic approach for GC patients. However, in other GC cases, low expression of E-cadherin could be initiated by other genomic factors, such as mutations or promoter methylation (46).

E-cadherin functions as a junction adhesion protein and is known to recruit β-catenin to the plasma membrane, where both molecules form a complex that plays a pivotal role in epithelial cell–cell adhesion. Disruption of this complex results in the loss of intercellular adhesion and induces cellular morphological changes, EMT, and progression to metastasis (47). In this study, *ARID1A* silencing in GC cells induced a reduction of E-cadherin expression, accompanied by obvious morphological alterations. This observation suggests that an EMT transformation might occur along with the increased migration abilities of GC cell lines. We found that the downregulation of E-cadherin by *ARID1A* silencing did not alter

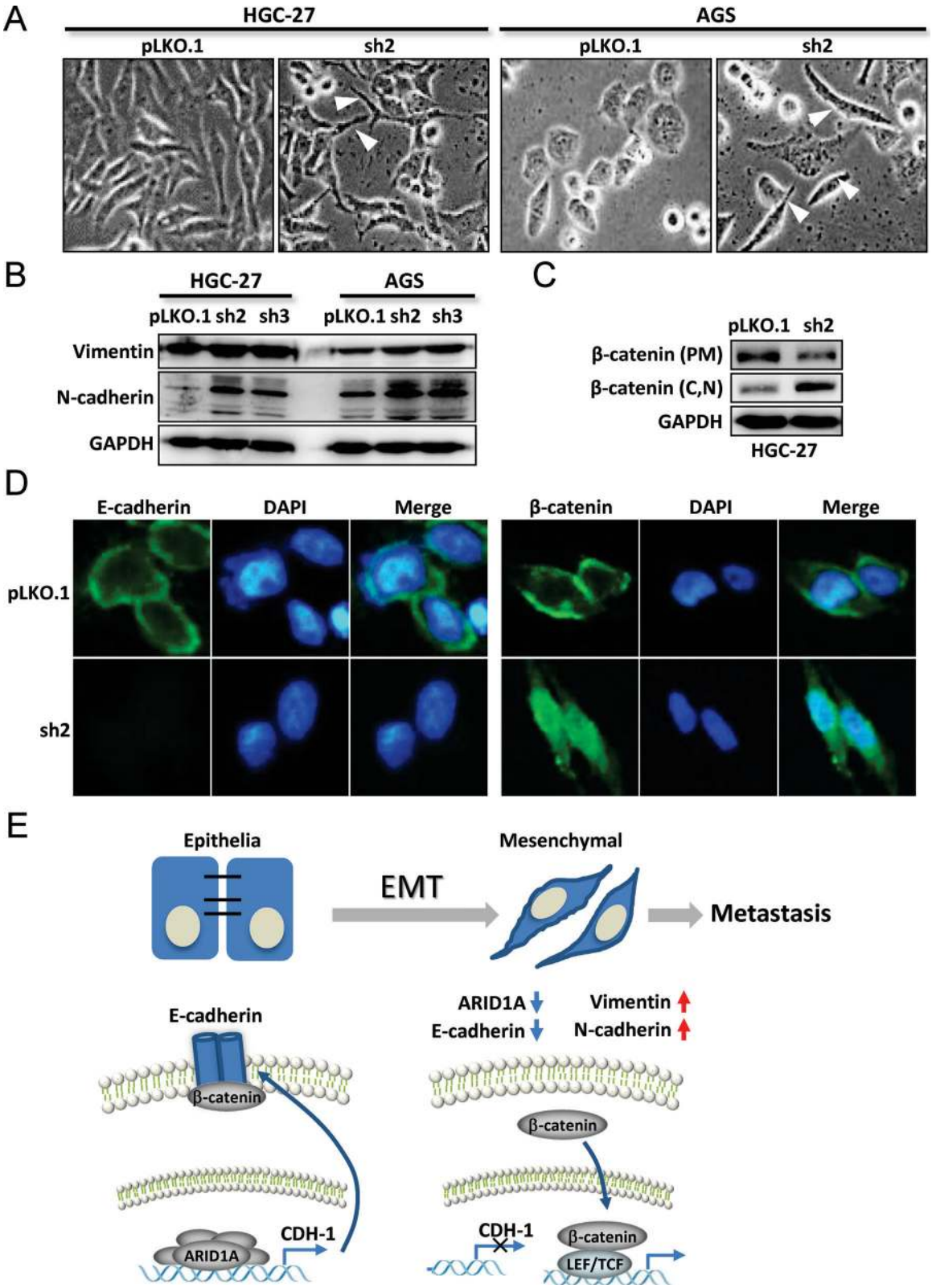

Fig. 5. Knockdown of *ARID1A* induces EMT of GC cells and the relocation of β-catenin. (**A**) *ARID1A* knockdown in HGC-27 and AGS cells induced morphological changes from routine round or polygon sharp shapes to spindle sharp shapes, indicating a potential EMT. Arrowheads illustrate shrunk cells with protruding filopodia or morphological changes. (**B**) Western blot results demonstrate that the expression of the mesenchymal markers vimentin and N-cadherin is elevated, suggesting an EMT transformation after *ARID1A* silencing in HGC-27 and AGS cells. (**C**) *ARID1A*-silenced HGC-27 cells were fractionated into plasma membrane and cytosol/nuclear fractions. Western blotting was performed using β-catenin. PM, plasma membrane fraction. C and N, cytoplasm and nucleus. (**D**) *ARID1A* was knocked down by shRNA in HGC-27 cells. Endogenous E-cadherin and β-catenin were stained by immunofluorescence with antibodies against both proteins, respectively. Nuclei were counterstained with DAPI. Membranous E-cadherin was almost diminished after *ARID1A* silencing, whereas β-catenin was redistributed from the plasma membrane to the cytoplasm and nucleus. (**E**) The molecular mechanism of ARID1A-associated SWI/SNF complex modulation of metastasis through regulation of E-cadherin/β-catenin association and the Wnt/β-catenin pathway.

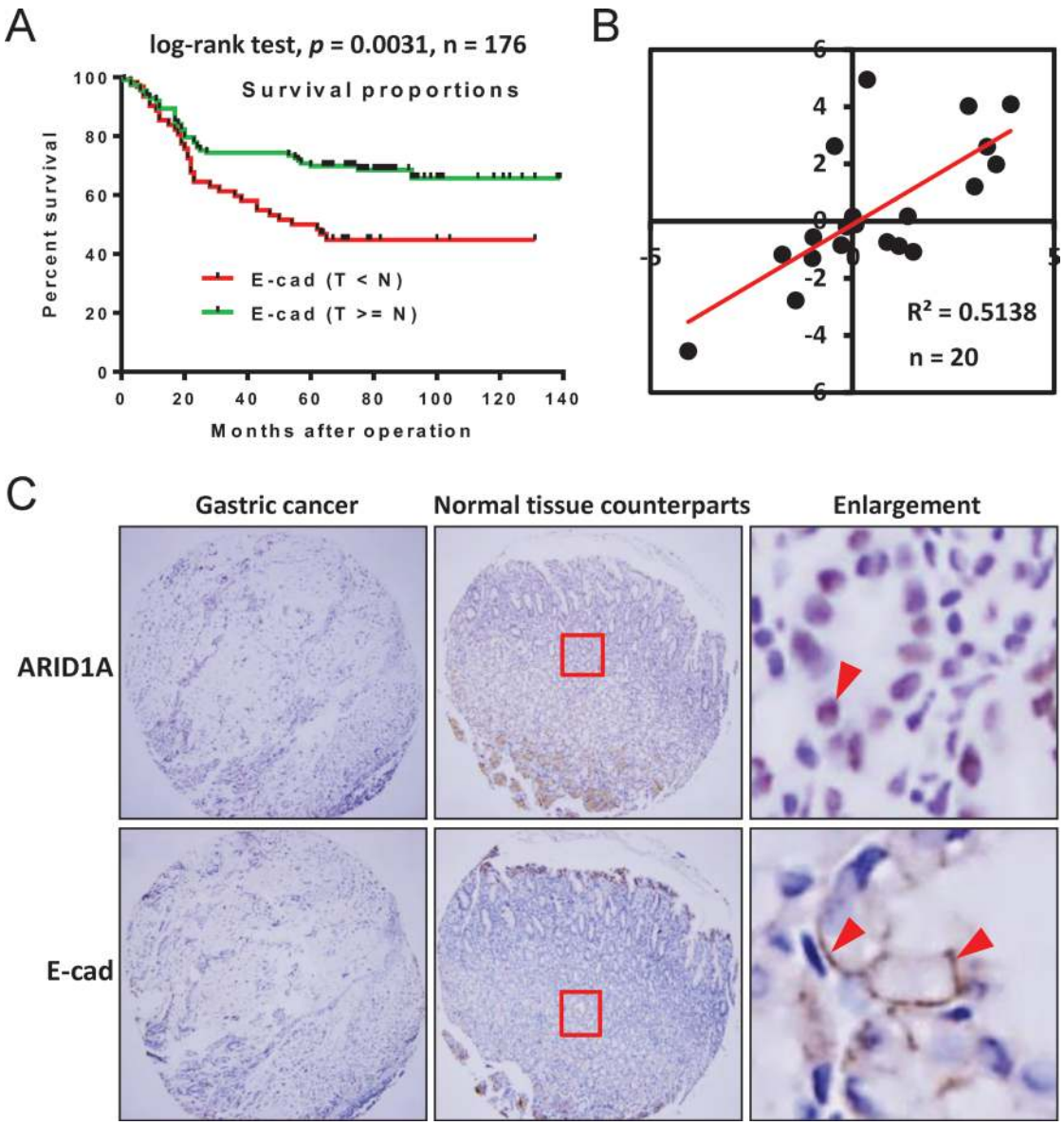

Fig. 6. Reduced expression of *ARID1A* and E-cadherin in gastric cancer tissues is associated with significantly worse clinical prognosis. (**A**) Kaplan–Meier survival curves of GC patients ($n = 176$) after gastrectomy. Patients with reduced E-cadherin expression had a significantly worse clinical prognosis than those with high BAF250a expression (log-rank test, $P = 0.0031$). (**B**) The expression level of both *ARID1A* and *CDH1* was evaluated by qPCR in 20 pairs of gastric carcinoma and adjacent normal gastric mucosa specimens collected from Zhongshan Hospital, Shanghai, China. Correlation coefficient (R^2) of both proteins was calculated as $\log_2$-transformed expression between normal and cancer tissues. (**C**) Two sets of tissue arrays containing sequential tissue sections from Zhongshan Hospital were stained by antibodies against BAF250a and E-cadherin. Images shown represent the cancerous section (first lane), normal counterpart (middle lane) and enlarged views of areas from the middle lane indicated with red boxes. BAF250a and E-cadherin expression were correlated. Increased nuclear staining of BAF250a was observed, whereas E-cadherin was expressed in the membranous portion of cell–cell junctions, as indicated by red arrow heads.

the expression level of β-catenin but induced a redistribution of β-catenin from the plasma membrane to the cytoplasm and nucleus, where β-catenin functions as an essential mediator of the canonical Wnt signaling pathway. This transformation of β-catenin is in consistent with the enhanced migration and invasion abilities of GC cells, as nuclear β-catenin expression is associated with invasion and metastasis (48).

In summary, we found that low expression of ARID1A and E-cadherin in GC is associated with poor prognosis and metastasis. ARID1A protein modulates *CDH1* transcription by interaction with its promoter. *ARID1A* silencing induces E-cadherin down-regulation and subcellular redistribution of β-catenin, enhancing GC cell migration and invasion. Consequently, *ARID1A* knockdown induces the morphological changes of GC cells and initiates an EMT process. ARID1A and E-cadherin were expressed in a synergetic fashion in GC tissues. Taken together, our findings suggest a novel molecular mechanism of *ARID1A* as a tumor suppressor for metastasis.

Supplementary material

Supplementary Table 1–5 and Figure 1 can be found at http://carcin.oxfordjournals.org/

Funding

Chinese National Key Program on Basic Research (973) Grant (2011CB910702, 2013CB911201); the National Key Program of Scientific Instrument Development Grant (2011YQ030139); the Shanghai Rising-Star Program Grant (11QH1400300).

Acknowledgements

We thank Dr Jian-Jun Du for providing the SGC-7901 cell line and Dr Qing-Hua Zhang for the AGS and GES-1 cell lines. H.B.Y., Q.Z., Y.H.J., Z.Q.T., and H.Z.F. performed the experiments. H.B.Y. and F.L. analyzed the data. X.F.W., Z.Q.T., and Y.H.S. provided the tissue array chip and tissue samples. Professor P.Y.Y. and F.L. conceived the study and F.L. wrote the paper.

Conflict of Interest Statement: None declared.

References

1. Roberts,C.W. *et al*. (2004) The SWI/SNF complex–chromatin and cancer. *Nat. Rev. Cancer*, **4**, 133–142.
2. Wilson,B.G. *et al*. (2011) SWI/SNF nucleosome remodellers and cancer. *Nat. Rev. Cancer*, **11**, 481–492.
3. Jones,S. *et al*. (2012) Somatic mutations in the chromatin remodeling gene ARID1A occur in several tumor types. *Hum. Mutat*., **33**, 100–103.
4. Wu,J.N. *et al*. (2013) ARID1A mutations in cancer: another epigenetic tumor suppressor? *Cancer Discov*., **3**, 35–43.
5. Wiegand,K.C. *et al*. (2010) ARID1A mutations in endometriosis-associated ovarian carcinomas. *N. Engl. J. Med*., **363**, 1532–1543.
6. Jones,S. *et al*. (2010) Frequent mutations of chromatin remodeling gene ARID1A in ovarian clear cell carcinoma. *Science*, **330**, 228–231.
7. Giulino-Roth,L. *et al*. (2012) Targeted genomic sequencing of pediatric Burkitt lymphoma identifies recurrent alterations in antiapoptotic and chromatin-remodeling genes. *Blood*, **120**, 5181–5184.
8. Guichard,C. *et al*. (2012) Integrated analysis of somatic mutations and focal copy-number changes identifies key genes and pathways in hepatocellular carcinoma. *Nat. Genet*., **44**, 694–698.
9. Fujimoto,A. *et al*. (2012) Whole-genome sequencing of liver cancers identifies etiological influences on mutation patterns and recurrent mutations in chromatin regulators. *Nat. Genet*., **44**, 760–764.
10. Huang,J. *et al*. (2012) Exome sequencing of hepatitis B virus-associated hepatocellular carcinoma. *Nat. Genet*., **44**, 1117–1121.
11. Sausen,M. *et al*. (2013) Integrated genomic analyses identify ARID1A and ARID1B alterations in the childhood cancer neuroblastoma. *Nat. Genet*., **45**, 12–17.
12. Imielinski,M. *et al*. (2012) Mapping the hallmarks of lung adenocarcinoma with massively parallel sequencing. *Cell*, **150**, 1107–1120.
13. Le Gallo,M. *et al*. (2012) Exome sequencing of serous endometrial tumors identifies recurrent somatic mutations in chromatin-remodeling and ubiquitin ligase complex genes. *Nat. Genet.*, **44**, 1310–1315.
14. Varela,I. *et al*. (2011) Exome sequencing identifies frequent mutation of the SWI/SNF complex gene PBRM1 in renal carcinoma. *Nature*, **469**, 539–542.
15. Gui,Y. *et al*. (2011) Frequent mutations of chromatin remodeling genes in transitional cell carcinoma of the bladder. *Nat. Genet*., **43**, 875–878.
16. Zhang,J. *et al*. (2013) Genetic heterogeneity of diffuse large B-cell lymphoma. *Proc. Natl. Acad. Sci. USA*, **110**, 1398–1403.
17. Streppel,M.M. *et al*. (2013) Next-generation sequencing of endoscopic biopsies identifies ARID1A as a tumor-suppressor gene in Barrett's esophagus. *Oncogene*. doi:10.1038/onc.2012.586.
18. Cancer Genome Atlas,N. (2012) Comprehensive molecular characterization of human colon and rectal cancer. *Nature*, **487**, 330–337.
19. Biankin,A.V. *et al*. (2012) Pancreatic cancer genomes reveal aberrations in axon guidance pathway genes. *Nature*, **491**, 399–405.
20. Wang,K. *et al*. (2011) Exome sequencing identifies frequent mutation of ARID1A in molecular subtypes of gastric cancer. *Nat. Genet*., **43**, 1219–1223.
21. Zang,Z.J. *et al*. (2012) Exome sequencing of gastric adenocarcinoma identifies recurrent somatic mutations in cell adhesion and chromatin remodeling genes. *Nat. Genet*., **44**, 570–574.
22. Guan,B. *et al*. (2011) ARID1A, a factor that promotes formation of SWI/SNF-mediated chromatin remodeling, is a tumor suppressor in gynecologic cancers. *Cancer Res*., **71**, 6718–6727.
23. Wang,D.D. *et al*. (2012) Decreased expression of the ARID1A gene is associated with poor prognosis in primary gastric cancer. *PLoS One*, **7**, e40364.
24. Mamo,A. *et al*. (2012) An integrated genomic approach identifies ARID1A as a candidate tumor-suppressor gene in breast cancer. *Oncogene*, **31**, 2090–2100.
25. Van Rechem,C. *et al*. (2009) HIC1 interacts with a specific subunit of SWI/SNF complexes, ARID1A/BAF250A. *Biochem. Biophys. Res. Commun*., **385**, 586–590.
26. Nagl,N.G. Jr *et al*. (2006) The c-myc gene is a direct target of mammalian SWI/SNF-related complexes during differentiation-associated cell cycle arrest. *Cancer Res*., **66**, 1289–1293.
27. Nagl,N.G. Jr *et al*. (2007) Distinct mammalian SWI/SNF chromatin remodeling complexes with opposing roles in cell-cycle control. *EMBO J*., **26**, 752–763.
28. Love,C. *et al*. (2012) The genetic landscape of mutations in Burkitt lymphoma. *Nat. Genet*., **44**, 1321–1325.
29. Zeng,Y. *et al*. (2013) ARID1A is a tumour suppressor and inhibits glioma cell proliferation via the PI3K pathway. *Head Neck Oncol*., **5**, 6.
30. Liang,H. *et al*. (2012) Whole-exome sequencing combined with functional genomics reveals novel candidate driver cancer genes in endometrial cancer. *Genome Res*., **22**, 2120–2129.
31. Sastry,L. *et al*. (2002) Titering lentiviral vectors: comparison of DNA, RNA and marker expression methods. *Gene Ther*., **9**, 1155–1162.
32. Cascio,S. *et al*. (2011) MUC1 protein expression in tumor cells regulates transcription of proinflammatory cytokines by forming a complex with nuclear factor-κB p65 and binding to cytokine promoters: importance of extracellular domain. *J. Biol. Chem*., **286**, 42248–42256.
33. Wang,X. *et al*. (2013) Clinical and prognostic implications of β1, 6-N-acetylglucosaminyltransferase V in patients with gastric cancer. *Cancer Sci*., **104**, 185–193.
34. He,H. *et al*. (2012) Snail is an independent prognostic predictor for progression and patient survival of gastric cancer. *Cancer Sci*., **103**, 1296–1303.
35. Abe,H. *et al*. (2012) ARID1A expression loss in gastric cancer: pathway-dependent roles with and without Epstein-Barr virus infection and microsatellite instability. *Virchows Arch*., **461**, 367–377.
36. Jang,B.G. *et al*. (2011) Molecular pathology of gastric carcinoma. *Pathobiology*, **78**, 302–310.
37. Zhao,C. *et al*. (2012) Promoter methylation of tumor-related genes in gastric carcinogenesis. *Histol. Histopathol*., **27**, 1271–1282.
38. Chandler,R.L. *et al*. (2013) ARID1a-DNA interactions are required for promoter occupancy by SWI/SNF. *Mol. Cell. Biol*., **33**, 265–280.
39. Kim,K. *et al*. (2002) Direct evidence for a role of beta-catenin/LEF-1 signaling pathway in induction of EMT. *Cell Biol. Int*., **26**, 463–476.
40. Müller,T. *et al*. (2002) Regulation of epithelial cell migration and tumor formation by beta-catenin signaling. *Exp. Cell Res*., **280**, 119–133.
41. Zhang,X. *et al*. (2012) Frequent low expression of chromatin remodeling gene ARID1A in breast cancer and its clinical significance. *Cancer Epidemiol*., **36**, 288–293.
42. Zhang,X. *et al*. (2013) Promoter hypermethylation of ARID1A gene is responsible for its low mRNA expression in many invasive breast cancers. *PLoS One*, **8**, e53931.
43. Bosse,T. *et al*. (2013) Loss of ARID1A expression and its relationship with PI3K-Akt pathway alterations, TP53 and microsatellite instability in endometrial cancer. *Mod Pathol.,* **26**, 1525–1535.
44. Skubitz,A.P. (2002) Adhesion molecules. *Cancer Treat. Res*., **107**, 305–329.
45. Xing,X. *et al*. (2013) The prognostic value of E-cadherin in gastric cancer: a meta-analysis. *Int. J. Cancer*, **132**, 2589–2596.
46. Zhang,K.L. *et al*. (2008) Increased frequency of CpG island methylator phenotype and CDH1 methylation in a gastric cancer high-risk region of china. *Transl. Oncol*., **1**, 28–35.
47. Wijnhoven,B.P. *et al*. (2000) E-cadherin-catenin cell-cell adhesion complex and human cancer. *Br. J. Surg*., **87**, 992–1005.
48. Suzuki,H. *et al*. (2008) Nuclear beta-catenin expression at the invasive front and in the vessels predicts liver metastasis in colorectal carcinoma. *Anticancer Res*., **28**, 1821–1830.

Received June 17, 2013; revised November 6, 2013; accepted November 9, 2013